

# Cold CO Gas in Protoplanetary Disks

Yuri Aikawa<sup>1</sup>

*Department of Earth and Planetary Sciences, Kobe University, Kobe 657-8501, Japan*

`aikawa@kobe-u.ac.jp`

## ABSTRACT

In a disk around DM Tau, previous observation of  $^{13}\text{CO}$  ( $J = 2 - 1$  and  $1 - 0$  transitions) derived the  $^{13}\text{CO}$  gas temperature of  $\sim 13 - 20\text{K}$ , which is lower than the sublimation temperature of CO (20 K). We argue that the existence of such cold CO can be explained by a vertical mixing of disk material. As the gas is transported from a warm layer to a cold layer, CO is depleted onto dust grains with a timescale of  $\sim 10^3$  yr. Because of the steep temperature gradient in the vertical direction, an observable amount of CO is still in the gas phase when the fluid parcel reaches the layer of  $\sim 13$  K. Apparent temperature of CO decreases as the maximum grain size increases from  $\mu\text{m}$ -size to mm-size.

*Subject headings:* stars: planetary systems: protoplanetary disks — stars: pre-main-sequence — ISM: molecules

## 1. Introduction

Theoretical models previously showed that the protoplanetary disks can be divided to three layers in the vertical direction from a chemical point of view (Aikawa & Herbst 1999; Willacy & Langer 2000; Aikawa et al. 2002; Bergin et al. 2006). Surface layer of the disk is a PDR (photon-dominated region) because of the interstellar UV, stellar UV, and stellar X-rays. As we go deeper into the disk, the radiation becomes weaker, and the density gets high enough to allow high abundances of organic molecules. In the midplane, on the other hand, heavy-element species are mostly depleted onto grains because of very high density and very low temperature. The three-layer model naturally explains the characteristics of the disk chemistry observed in radio wavelengths: low average abundances of gaseous organic species and relatively high abundances of radical species (ex. CN/HCN ratio) in comparison with the molecular clouds(Dutrey et al. 1997; Qi et al. 2003; Thi et al. 2004). Molecular emission lines arise mostly from the intermediate molecular layer, because it is chemically rich

and spans a density range that covers critical densities of many (sub-)millimeter rotational transitions.

Dartois et al. (2003) observed two rotational transitions ( $J = 2-1$  and  $1-0$ ) of various CO isotopes, from which they derived  $^{12}\text{CO}$  temperature to be 30 K and  $^{13}\text{CO}$  temperature 13 – 20 K. Since the  $^{13}\text{CO}$  lines trace the deeper layer of the disk than the  $^{12}\text{CO}$  lines, it was the first observational evidence that the gas temperature increases with height from the midplane at radii of  $r > 50$  AU, which are traced by the current radio telescopes. In addition, the  $^{13}\text{CO}$  temperature challenges the theoretical model; since the sublimation temperature of CO is  $\sim 20$  K, a layer with  $T \sim 13 - 20$  K is considered to be the freeze-out layer.

Recently, Aikawa & Nomura (2006) briefly argued that existence of such cold CO can be explained by vertical mixing due to turbulence. In the vertical direction gas can migrate over  $\sim 10$  AU in the vertical direction, and thus can travel from the  $T = 20$  K layer to the  $T = 13$  K layer within  $10^4$  yr, which is comparable to a freeze-out timescale in the DM Tau disk. In this paper, we examine their arguments in more detail using various disk models. The rest of the paper is organized as follows. In §2, we derive a typical migration length of material within the freeze-out timescale of CO. In §3, a distance between the  $T = 13$  K and 20 K layers is measured in various disk models, and is compared with the migration length. We compare our results with the recent numerical calculation of turbulent disk chemistry in §4. Summary is contained in §5.

## 2. Basic Equations

Following Willacy et al. (2006), we consider a vertical mixing in the disk. The net transport flux of species  $i$  by the turbulent diffusion is

$$\phi(i) = -Kn(\text{H}_2) \frac{dx(i)}{dz}, \quad (1)$$

where  $x(i)$  is the abundance of species  $i$  relative to the number density of hydrogen molecule  $n(i)/n(\text{H}_2)$ . We assume that the diffusion coefficient  $K$  is equal to the viscosity coefficient:  $K \equiv < v_t l > = \alpha c_s h$  where  $v_t$  is the turbulent velocity,  $l$  is the mixing length,  $\alpha$  is the alpha-viscosity parameter (Shakura & Sunayev 1973),  $c_s$  is the sound velocity, and  $h$  is the scale height of the disk. The chemical continuity equation is

$$\frac{\partial n(i)}{\partial t} + \frac{\partial \phi(i)}{\partial z} = P_i - L_i \quad (2)$$

where  $P_i$  and  $L_i$  are the chemical production and loss terms for species  $i$ .

We now consider the steady-state abundance distribution of CO near the boundary between the warm molecular layer and freeze-out layer. Since CO is the most abundant and stable species among the carbon-bearing species in the warm molecular layer, the main production and loss terms are desorption from and adsorption onto grains, respectively. As the matter is transported from the warm molecular layer to the freeze-out layer, the desorption term becomes negligible. Hence the vertical distribution of CO is determined by the diffusion from the warm molecular layer and the adsorption onto grains, i.e.

$$\frac{d\phi(\text{CO})}{dz} = -\pi a^2 S \sqrt{\frac{8kT}{\pi m(\text{CO})}} n_g n(\text{CO}) \quad (3)$$

where  $a$  is the grain radius,  $S$  is the sticking probability,  $k$  is the Boltzman constant,  $m(\text{CO})$  is the mass of CO molecule, and  $n_g$  is the grain number density. In order to derive an analytic solution, we neglect the density gradient ( $dn(\text{H}_2)/dz$ ), which is justified because the abundance gradient is steeper than the density gradient. Then the basic equation is reduced to

$$K \frac{d^2 x(\text{CO})}{dz^2} = \pi a^2 S \sqrt{\frac{8kT}{\pi m(\text{CO})}} n_g x(\text{CO}). \quad (4)$$

The analytic solution for this equation is

$$x = x_0 \exp\left(-\frac{z_0 - z}{\lambda}\right) \quad (5)$$

where  $x_0$  is the canonical CO abundance ( $10^{-4}$ ) in the warm molecular layer and  $z_0$  is the height of  $T = 20$  K layer, i.e. the boundary between the warm molecular layer and freeze-out layer. The decay length  $\lambda$  is given by

$$\lambda = \left( \frac{\pi a^2 S}{\alpha c_s h} \sqrt{\frac{8kT}{\pi m(\text{CO})}} n_g \right)^{-1/2}. \quad (6)$$

In other words, material can migrate from the boundary  $z = z_0$  to  $z = z_0 - \lambda$  within the freeze-out timescale of CO.

### 3. Results

In this section, we evaluate  $\lambda$  in various disk models. Considering the vertical temperature gradient, we discuss if the turbulence can transport observable amount of CO to the  $T < 20$  K layer.

### 3.1. Migration length of CO and vertical temperature gradient

The decay length  $\lambda$  is determined by the ratio between the rate coefficient of adsorption and diffusion coefficient. The former depends on temperature, sticking probability, and total grain surface area. Temperature is set to be 17 K, since we are interested only in a region between 13 K and 20 K, and since the dependence of  $\lambda$  on temperature is not strong. Sticking probability  $S$  is set to be 0.5. As for dust grains, we assume dust/gas mass ratio of 1% and grain radius of  $10^{-5}$  cm. The number density of grain  $n_g$  is then  $1.6 \times 10^{-12} n_H$ , where  $n_H$  is the number density of hydrogen nuclei. If the grain size distribution follows the MRN model (Mathis et al. 1997), the total surface area ( $\int \pi a^2 n_g(a) da$ ) of dust grains should be about three times larger than assumed in our model. However, observations suggest that the dust grains in disks are larger than the interstellar dust (D'Alessio et al. 2001; Rodmann et al. 2006). Dependence of our results on grain size in disks will be discussed in the next subsection.

The diffusion coefficient depends on  $\alpha$  and scale height. We assume  $\alpha = 0.01$ . Analyzing the CO emission lines in DM Tau disk, Guilloteau & Dutrey (1998) found the intrinsic local velocity dispersion is essentially thermal, with a turbulent component of  $0.05 \text{ km s}^{-1} < v_t < 0.11 \text{ km s}^{-1}$ , while Dartois et al. (2003) estimate  $v_t \sim 0.16 \text{ km s}^{-1}$ . Thus by setting  $\alpha = 0.01$ , we assume the mixing length  $l$  of several  $10^{-2} h$ . The scale height of the disk is given by

$$h = \sqrt{\frac{2kTr^3}{GM_*\mu m_H}}, \quad (7)$$

where  $\mu$  is the mean molecular weight,  $m_H$  is the hydrogen mass,  $G$  is the gravitational constant, and  $M_*$  is the mass of the central star. We assume  $\mu = 2.34$  and  $M_* = 0.5M_\odot$ . Then  $\lambda$  is given as a function of hydrogen number density  $n_H$  and disk radius  $r$ :

$$\lambda = \left( 1.6 \times 10^{-12} \frac{2\pi a^2 S}{\alpha c_s} \sqrt{\frac{GM_*\mu m_H}{\pi m(\text{CO})r^3}} n_H \right)^{-1/2}. \quad (8)$$

Here we evaluate  $\lambda$  in two disk models from literature: DM Tau disk model, which is constructed to fit the SED assuming the grain size of  $0.1 \mu\text{m}$  (Ceccarelli et al. 2005), and a model by D'Alessio et al. (1999), who assumed interstellar-type dust is well mixed with gas. Models give  $n_H$  and  $T$  as a function of  $r$  and  $z$ . At each radius we calculate  $\lambda$  using  $n_H$  in the layer of  $T = 13 - 20$  K. In Figure 1, asterisks, open boxes, and crosses depict  $\lambda$  with the density  $n_H$  at  $T = 20$  K layer,  $T = 13$  K layer, and with the average density of  $T = 13 - 20$  K layer at each radius, respectively. The black marks are the DM Tau disk model and the gray marks are the D'Alessio et al. (1999) model. For example,  $n_H$  is  $\sim 10^7$

$\text{cm}^{-3}$  at the boundary between the molecular layer and the freeze-out layer at  $r \sim 400$  AU in both models. Then the decay length  $\lambda$  is  $\sim 10$  AU.

Also shown in Figure 1 (closed circles) is the distance between the layers of  $T = 20$  K and 13 K,  $dz_{20-13}$ , at each radius in the two disk models. It can be seen that at radius of  $> 400$  AU,  $dz_{20-13}$  is about 4 times larger than  $\lambda$ . In other words, when the disk material transported vertically from the 20 K layer to the 13 K layer, gaseous CO is  $e^{-4}$  times the canonical value.

It should be noted that the column density of CO gas with  $T < 20$  K is given by  $\lambda n_0(\text{CO})$ , where  $n_0(\text{CO})$  is the number density of CO molecule at the 20 K layer ( $z = z_0$ ). At the radius of 400 AU, for example,  $\lambda$  is about 10 AU, and  $n_0(\text{CO})$  is  $\sim 10^3 \text{ cm}^{-3}$ . Then the column density of  $^{12}\text{CO}$  with  $T < 20$  K is  $\sim 10^{17} \text{ cm}^{-2}$ , which corresponds to the opacity of  $\tau \sim 1$  for the  $J = 1 - 0$  emission line of  $^{13}\text{CO}$ , assuming the isotope abundance ratio of  $n(^{12}\text{CO})/n(^{13}\text{CO}) = 60$ . Therefore, the amount of cold  $^{13}\text{CO}$  produced by the turbulent mixing is high enough to account for the observation by Dartois et al. (2003).

Finally, it is obvious from the equation (6) that in the disks with larger (smaller)  $\alpha$ ,  $\lambda$  is larger (smaller), and thus the cold CO is more (less)abundant.

### 3.2. Effect of grain growth

So far, we have assumed that dust grains in disks are similar to the interstellar grains. However, observations suggest grains in disks are larger than the interstellar grains. Dust lane width of edge-on disks is smaller than that of model disks with interstellar grains. The SED is better reproduced by the disk models with the maximum grain radius in millimeter range (D'Alessio et al. 2001). In this subsection, we compare the decay length  $\lambda$  and the vertical temperature gradient in the disk models of Aikawa & Nomura (2006). They investigated the effect of grain growth on disk structure ( $n_{\text{H}}$  and  $T$ ); the number density of grains with radius  $a$  is assumed to be proportional to  $a^{-3.5}$ , and the maximum size  $a_{\text{max}}$  is varied with the dust/gas mass ratio fixed.

Figure 2 compares  $\lambda$  and  $dz_{20-13}$  in the models with (a)  $a_{\text{max}} = 10\mu\text{m}$  and (b) 1 mm. Compared with the case of uniform grain size ( $0.1\mu\text{m}$ ), the total surface area of grains is smaller by a factor of (a) 0.3 and (b) 0.03. Because of the smaller total surface area of grains, the adsorption time scale and thus  $\lambda$  are larger in the model with  $a_{\text{max}} = 1$  mm (see eq. 6). On the other hand,  $dz_{20-13}$  is smaller in  $a_{\text{max}} = 1$  mm model than in  $a_{\text{max}} = 10\mu\text{m}$  model at  $r > 100$  AU. Temperature in the disk atmosphere is lower, and hence the vertical width of the disk is smaller in the model with larger  $a_{\text{max}}$ , because of the reduced number of

small grains which mainly contribute to the absorption of stellar light. At  $r = 100$  AU, the temperature in the midplane layer increases with grain growth, and  $dz_{20-13}$  is slightly larger in the  $a_{\max} = 1$  mm model. We can conclude that at  $r > 100$  AU the amount of cold CO gas increases as the  $a_{\max}$  increases from  $10\mu\text{m}$  to 1 mm.

#### 4. Discussion

Recently Semenov et al. (2006) investigated the molecular evolution in a turbulent disk by coupling the chemical reaction network and turbulent diffusion. They showed that the two-dimensional diffusion increases the amount of cold CO, but the amount is too small to account for the observation by Dartois et al. (2003). Why is the cold CO much less abundant in their model than estimated in the present work?

We suspect that the deficiency of cold CO is caused by the too efficient grain-surface reactions. Even in the  $T \sim 20$  K region in their static model, CO abundance is much smaller than the canonical value. Inclusion of the vertical diffusion *reduces* the cold CO, because more CO is converted to  $\text{H}_2\text{CO}$  by grain-surface reactions (see their §3). Since the sublimation temperature of  $\text{H}_2\text{CO}$  is higher than that of CO, the hydrogenation depletes CO at  $T \sim 20$  K. The rate of hydrogenation, however, seems to be overestimated in their model, as discussed below.

In the layer of  $T \sim 20$  K at  $r > 100$  AU, we estimate the number density of H atoms (not included in  $\text{H}_2$ ) in the gas phase to be  $n(\text{H}) \lesssim 10 \text{ cm}^{-3}$ , referring to the model of Aikawa & Nomura (2006) with  $a_{\max} = 10\mu\text{m}$ . The number of H atoms accreting onto a grain with radius  $a$  is

$$\sqrt{\frac{8kT}{\pi m(\text{H})}} n(\text{H}) \pi a^2 = 2 \times 10^{-4} \left( \frac{T}{20\text{K}} \right)^{1/2} \left( \frac{a}{0.1\mu\text{m}} \right)^2 \text{s}^{-1}. \quad (9)$$

The desorption rate, on the other hand, is

$$\sqrt{\frac{2n_s E_{\text{D}}}{\pi^2 m(\text{H})}} \exp\left(-\frac{E_{\text{D}}}{kT}\right), \quad (10)$$

where  $n_s$  is the number density of adsorption sites on a grain ( $\sim 1.5 \times 10^{15} \text{ cm}^{-2}$ ), and  $E_{\text{D}}$  is the adsorption energy (Herbst 1993). If  $E_{\text{D}}$  is 350 K (Hasegawa & Herbst 1993), the desorption rate is  $7.4 \times 10^4 \text{ s}^{-1}$  at 20 K. Hence a number of H atoms on a dust grain is much smaller than unity even for grains with  $a = 10\mu\text{m}$ . With such a low H atom abundance on a grain, the hydrogenation rate is limited by the accretion rate rather than determined

by a migration rate on a grain (Caselli et al. 1998). According to the model description of Semenov et al. (2006), they seems to have estimated the hydrogenation rate using the migration rate, which can be an overestimate.

Reality can be more complex than the above argument. For example, grains are not spherical but would be porous, which will enhance the possibility of reaction before desorption (Perets & Biham 2006). On the other hand, laboratory experiment suggests that CO is hydrogenated only in the surface layer of the ice mantle (Watanabe et al. 2003). Most of the currently-available astrochemistry models may overestimate the hydrogenation rates, since they do not discriminate the surface species from species inside ice mantle. Modeling the grain-surface reactions is still a challenging subject in the astrochemical studies.

However, it is an observational fact that cold ( $\sim 13$  K) CO gas exists in the disk. If the CO depletion is caused by hydrogenation in the model by Semenov et al. (2006), it tells us even the abundance of simple gaseous species can be dependent on how we model the grain-surface reactions – an important caution for future models.

## 5. Summary

We have shown that in protoplanetary disks the turbulent diffusion can produce observable amount of CO that is colder than the sublimation temperature. As disk material is transported to the layer with  $T < 20$  K, freeze out proceeds with timescale of  $\sim 10^3 (n_{\text{H}}/10^7 \text{ cm}^{-3})$ . Since the gas migrates over a distance of  $\sim 10$  AU within this timescale, CO gas of column density  $\sim 10^{17} \text{ cm}^{-2}$  exists in the cold ( $T < 20$  K) layers, which explains the observation by Dartois et al. (2003). As the dust grains in the disk become larger by coagulation, the freeze-out time scale increases, and the vertical temperature gradient at  $T \sim 20$  K gets steeper. Hence, the apparent CO temperature decreases as the maximum grain size increases from  $\mu\text{m}$ -size to mm-size.

I thank referees for their comments which were helpful in improving the manuscript. I am grateful to C. Ceccarelli, C. Dominik, P. D'Alessio and H. Nomura for providing their disk models. This work is supported by a Grant-in-Aid for Scientific Research (16036205, 17039008) and “The 21st Century COE Program of Origin and Evolution of Planetary Systems” of the Ministry of Education, Culture, Sports, Science and Technology of Japan (MEXT).

## REFERENCES

Aikawa, Y. & Herbst, E. 1999, *A&A*, 351, 233

Aikawa, Y. & Nomura, H. 2006, *ApJ*, 642, 1152

Aikawa, Y., van Zadelhoff, G. J., van Dishoeck, E. F., & Herbst, E. 2002, *A&A*, 386, 622

Bergin, E. A., Aikawa, Y., van Dishoeck, E. F., & Blake, G. A. 2006, in *Protostars and Planets V*, ed. B. Reipurth (Tucson: Univ. Arizona Press), in press

Caselli, P., Hasegawa, T. I., & Herbst, E. 1998, *ApJ*, 495, 309

Ceccarelli, C., Dominik, C., Caux, E., Lefloch, B., & Caselli, P. 2005, *ApJ*, 631, L81

D'Alessio, P., Calvet, N., Hartmann, L., Lizano, S., & Cantó, J. 1999, *ApJ*, 527, 893

D'Alessio, P., Nuria, C., & Hartmann, L. 2001, *ApJ*, 553, 321

Dartois, E., Dutrey, A., & Guilloteau, S. 2003, *A&A*, 399, 773

Dutrey, A., Guilloteau, S., Guélin, M. 1997, *A&A*, 317, L55

Guilloteau, S. & Dutrey, A. 1998, *A&A* 339, 467

Hasegawa, T. I., & Herbst, E. 1993a, *MNRAS*, 261, 83

Herbst, E. 1993, in *Dust and Chemistry in Astronomy*, eds. Millar, T. J., & Williams, D. A. (Institute of Physics Publishing), p. 183

Mathis, J. S., Rumpl, W., & Nprdsieck, K. H. 1977, *ApJ*, 217, 425

Perets, H. B. & Biham, O. 2006, *MNRAS*, 365, 801

Qi, C., Kessler, J. E., Koerner, D. W., Sargent, A. I., & Blake, G. A. 2003, *ApJ*, 597, 986

Rodmann, J., Henning, Th., Chandler, C.J., Mundy, L., & Wilner, D.J. 2006, *A&A*, 446, 211

Semenov, D., Wiebe, D., & Henning, Th. 2006, *ApJL*, in press

Shakura, N.I. & Sunyaev, R.A. 1973, *A&A* 24, 337

Thi, W. F., van Zadelhoff, G. J., & van Dishoeck, E. F. 2004, *A&A*, 425, 955

Watanabe, N., Shiraki, T. & Kouchi, A. 2003, *ApJL*, 588, L121

Willacy, K., & Langer, W. D. 2000, ApJ, 544, 903

Willacy, K., Langer, W., Allen, M., & Bryden, G. 2006, ApJ, 644, 1202

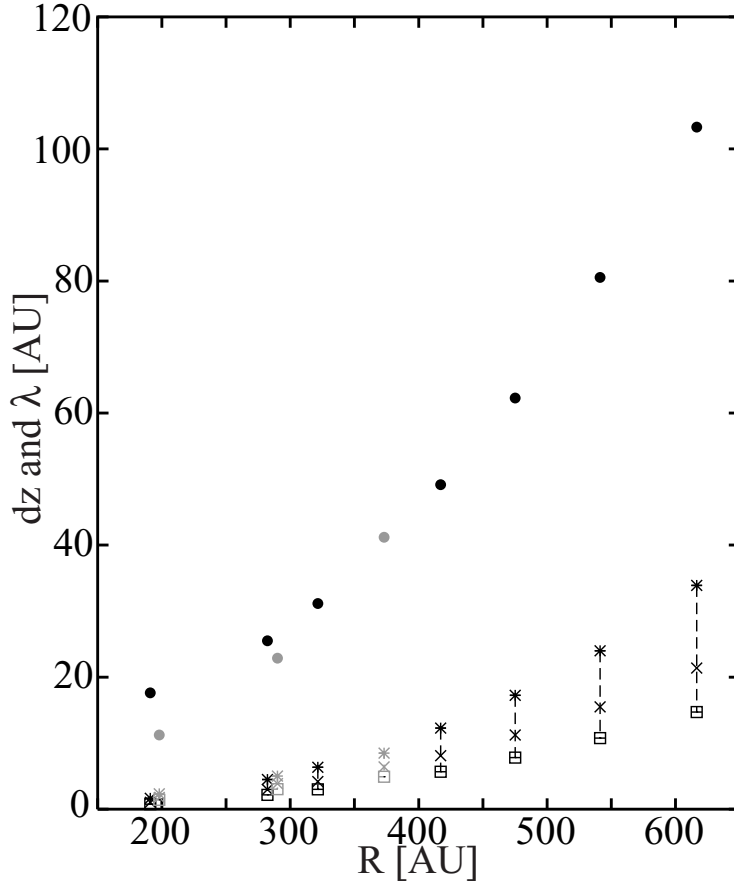


Fig. 1.— The black marks depict DM Tau disk model by Ceccarelli. et al. (2005), while the gray marks are the disk model by D'Alessio et al. (1999) with the accretion rate of  $10^{-8} M_{\odot} \text{ yr}^{-1}$ . Asterisks, open boxes, and crosses depict  $\lambda$  with the density  $n_{\text{H}}$  at  $T = 20 \text{ K}$  layer,  $T = 13 \text{ K}$  layer, and with the average density of  $T = 13 - 20 \text{ K}$  layer at each radius, respectively. In the DM Tau disk model, for example, the densities  $n_{\text{H}}$  at  $T = 13 \text{ K}$  and  $20 \text{ K}$  layers are  $6.6 \times 10^6 \text{ cm}^{-3}$  and  $1.2 \times 10^6 \text{ cm}^{-3}$  at  $r = 616 \text{ AU}$ , while they are  $4.2 \times 10^8 \text{ cm}^{-3}$  and  $9.1 \times 10^7 \text{ cm}^{-3}$  at  $r = 191 \text{ AU}$ , respectively. Closed-circles depict the distance between the layers of  $T = 20 \text{ K}$  and  $13 \text{ K}$  ( $dz_{20-13}$ ).

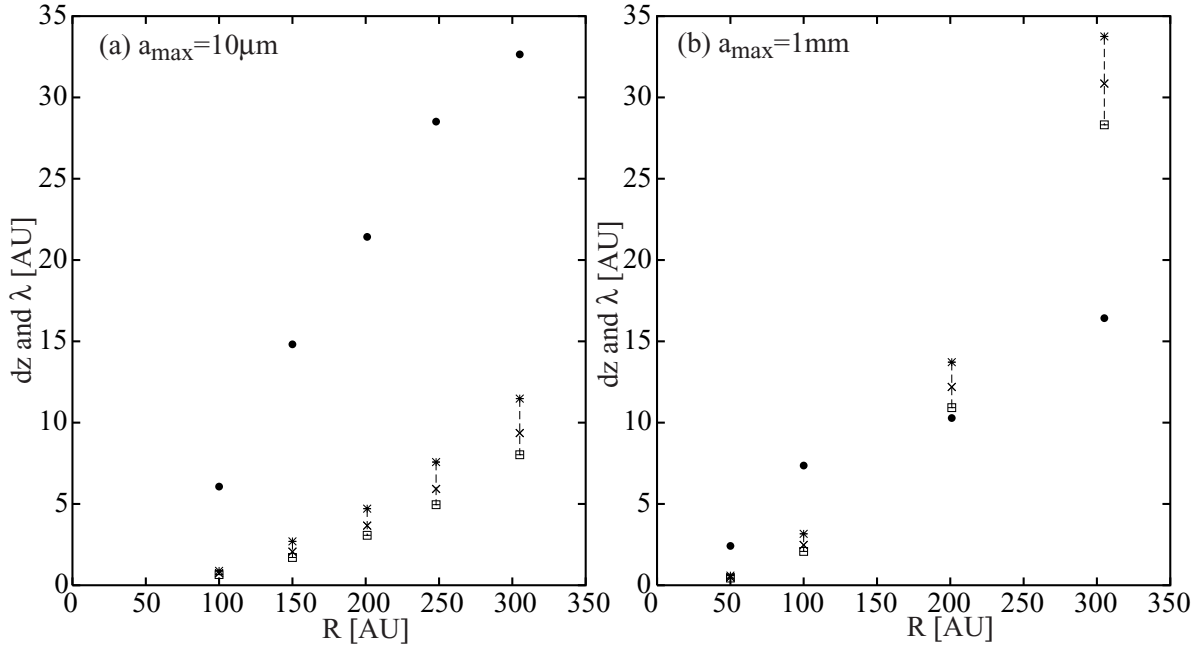


Fig. 2.— Decay length of CO abundance  $\lambda$  and distance between the layers of  $T = 20 \text{ K}$  and  $13 \text{ K}$  ( $dz_{20-13}$ ) as in Figure 1. Disk models are by Aikawa & Nomura (2006) with the maximum grain size of  $10 \mu\text{m}$  (a) and  $1 \text{ mm}$  (b). In the model with  $a_{\max} = 10 \mu\text{m}$  (a), the densities  $n_{\text{H}}$  at  $T = 13 \text{ K}$  and  $20 \text{ K}$  layers are  $2.4 \times 10^7 \text{ cm}^{-3}$  and  $1.2 \times 10^7 \text{ cm}^{-3}$  at  $r = 305 \text{ AU}$ , while they are  $6.8 \times 10^8 \text{ cm}^{-3}$  and  $3.7 \times 10^8 \text{ cm}^{-3}$  at  $r = 100 \text{ AU}$ , respectively. In the model with  $a_{\max} = 1 \text{ mm}$  (b), the density  $n_{\text{H}}$  at  $T = 13 \text{ K}$  and  $20 \text{ K}$  layers are  $1.9 \times 10^7 \text{ cm}^{-3}$  and  $1.4 \times 10^7 \text{ cm}^{-3}$  at  $r = 305 \text{ AU}$ , while they are  $5.2 \times 10^9 \text{ cm}^{-3}$  and  $2.9 \times 10^9 \text{ cm}^{-3}$  at  $r = 50 \text{ AU}$ , respectively.